Aerodynamic Research on Lifting Surfaces and Performance for Micro & Mini UAV

Thierry Keuter ; Davy Hermans ; Dimitri Jérôme : Research Engineers
Prof. Dr. Roland Decuypere : Project Coordinator
Royal Military Academy
Department of Mechanics (MAPP)
30 Renaissance Avenue
B-1000 Brussels, Belgium
Tel & Fax : +32 2 737 65 50
Email : Roland.Decuypere@mapp.rma.ac.be

Guy Boyet, ONERA Palaiseau, Chemin de la Hunière,
F-91761 Palaiseau Cedex
Tel : +33 1 69 93 62 45 ; Fax : +33 1 69 93 63 00
Email : boyet@onera.fr

Résumé— **This paper presents the first steps of a research program aiming to develop a mini/micro UAV (MAV) at the Royal Military Academy of Belgium. In this early stage, the research is mainly focused on the visualization, measurement and calculation of the flow field around airfoils at low Reynolds numbers (Re). The first part gives a brief outline of the specifications of a MAV and explains how they can contribute to military and civil missions. Measurements obtained by an aerodynamic balance, on an Eppler 61 airfoil are presented in the second part and compared to the results published by Professor Thomas Mueller from the University of Notre Dame, USA. Another section deals with flow field measurements performed by Laser Doppler Velocimetry (LDV). Subsequently, in order to obtain a more complete image of the flow field of a MAV, the pressure distribution around the airfoil was also measured. Finally, a conceptual design elaborated in collaboration with ONERA, France, is presented.**

I. Introduction

THE final goal of the ongoing research is to design and build a mini UAV with a range between 3 and 10 km and an autonomous flight of 20 to 60 minutes. The presence of onboard intelligence is of first importance. The plane is to be pre-programmed, using a laptop, to overfly a number of waypoints and send real-time images to the user. Thus, in contrast with radio controlled aerial vehicles, navigation by use of a joystick is out of the question. Another very important feature concerns the overall dimensions of the mini UAV. The airplane (including the ground station) should be easy to carry by one person. If the size of the plane is such that it needs to be dismantled for transport, the time needed for reassembling should be limited to a few minutes.

Military applications include reconnaissance and surveillance, target identification, target designation, sensor emplacement, sensing of nuclear, biological and chemical contaminants, pilot recovery assistance, jamming, communication relay, minefield identification, flash detection of artillery fire ... Envisioned civil operations are counter drug support, police assistance in cases where hostages are held and assistance in finding survivors after disasters like earthquakes, volcano eruptions, forest or bush fires, flooding etc ...

Some of the biggest challenges encountered in the design of micro and mini UAV concern the low Reynolds numbers [1]. Flows around full size airplanes are characterized by Reynolds numbers of a few millions whereas sizes and velocities associated with MAV lead to Reynolds numbers below two hundred thousand and may be as low as a few ten thousand. At Re below 500,000 boundary layer behavior with associated separation bubbles is very complicated and up to now, no mathematical or theoretical analyses has been able to deal adequately with it. As a consequence, fundamental experimental research is necessary.

For this purpose we have at our disposal an improved wind tunnel facility. The main features are a capacity of 23 kW, a transparent square test section of 460 mm wide, and a maximum flow velocity of 35 m/s.

II. FORCE MEASUREMENT

A. *Characteristics of the balance*

Several changes were needed in order to improve some characteristics of our wind tunnel facility. We performed force measurement on the Eppler 61 airfoil, which is a thin, highly cambered profile intended for free-flight duration models. The reason why this airfoil was selected was mainly that Thomas Mueller from the University of Notre Dame [2], extensively describes its aerodynamic behavior.

The standard aerodynamic balance (figure 1) was equipped with three strain gauges with following features:

- Rated capacity : 220 N
- Non Linearity error : ± 0.03% full scale
- Hysteresis error : ± 0.02 % full scale

Flexible cables to strain gauge load cells, measuring the fore and aft lift forces and the drag force, transmit the forces acting on the force plate. The drag cable, which lies horizontally, acts on a line through the center of the model support, while the two lift cables act vertically through points disposed equidistant from the center of the model support and in the same horizontal plane as the support.

The sum of the forces on the fore and aft lift cables gives the lift on the model, while the difference is proportional to the pitching moment.

A stepper motor (figure 1) has been added to the aerodynamic balance in order to improve significantly the accuracy of the position of the model.

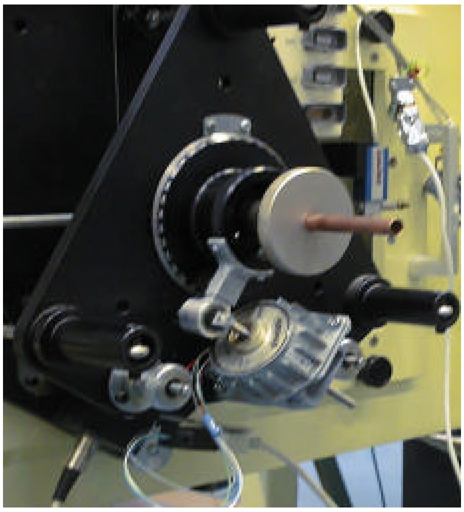

Figure 1: Balance with motorized chuck

Early experiments have shown that the original data acquisition system was inaccurate. A new system has been developed incorporating digital conditioning and programmable sampling modules. A new completely transparent test section has also been built.

The entire force measurement system is represented on figure 2.

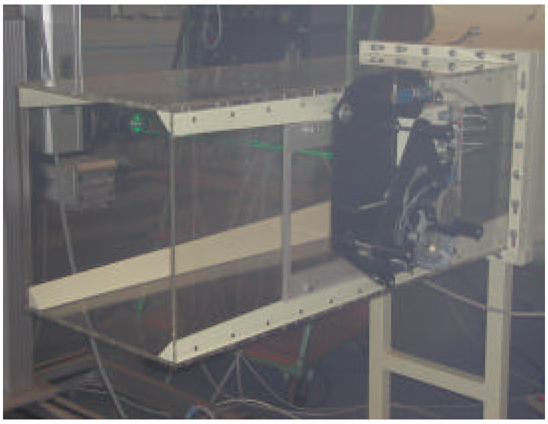

Figure 2: Working Section with Aerodynamic Balance

B. *Comparison of results*

As mentioned previously, we wanted to validate our wind tunnel facility. Actually, any wind tunnel has various defects, which cannot be entirely removed. The model, for instance, tends to block the flow through the test section and this blocking effect varies with the angle of attack. If there are any supporting struts or wires, an estimate on their effect has to be made. When balances are used, there are often small gaps, which may possibly disturb the flow at the ends of the tunnel model. There are problems caused by interference of the boundary layers in the corners of the test section. For all these and other reasons, including inaccuracies in manufacturing the models, the results reported from one wind tunnel always differ to some extent from those obtained elsewhere.

Professor Mueller's knowledge in the field of aeronautics hasn't to be underlined anymore. That's why, with his permission, we performed force measurement on an Eppler 61 airfoil (figure 3) at several Reynolds numbers: 42.000, 46.000, 63.500, 87.000 and compared our results with the ones published in ref [2]. The profile tested at the Royal Military Academy (RMA) is machined in aluminum, with a chord of 140 mm and a wingspan of 460 mm, being the test section width. It's the theoretical infinite span state, which is described as 'two dimensional'.

Figure 4 displays our results represented in a polar diagram. Knowing that usually, comparison of results obtained in different wind tunnels, is most critical at the lowest Re, detailed comparison between the RMA and Notre Dame results is given for Re = 42,000.

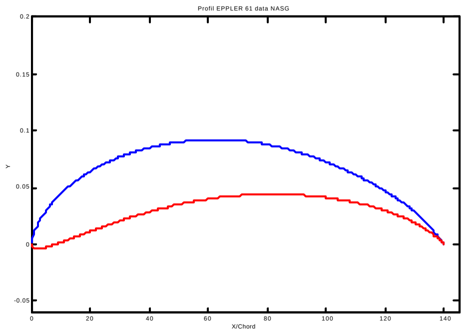

Figure 3 : Eppler 61 airfoil

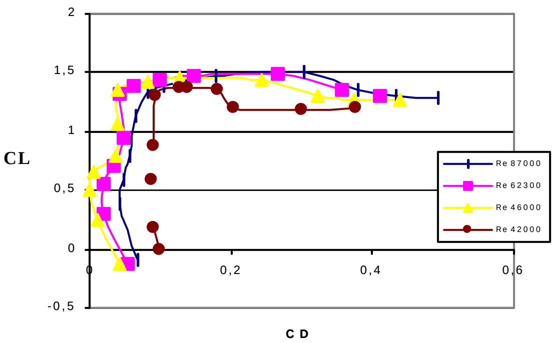

Figure 4 : Polar Curves Eppler 61
Re 42,000 – 46,000 – 62,300 – 87,000

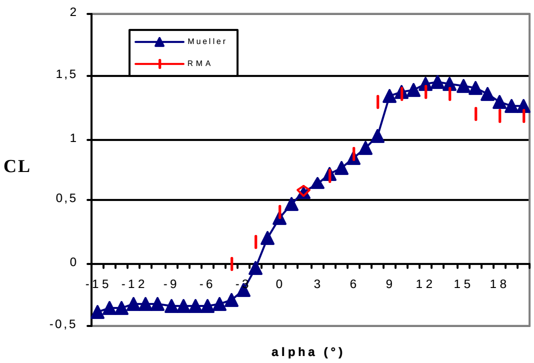

Figure 5 : Lift Curves Re 42,000
Notre Dame – R M A

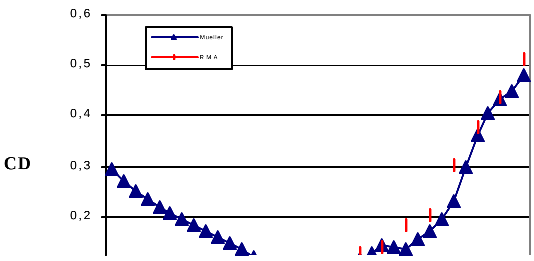

It's expected that the polar curves shift to the right with decreasing Reynolds number. However, for Re = 62,300 and Re = 87,000 this seems not to be the case. Detailed analysis of several parameters indicated that this anomaly was provoked by an insufficient precision of the measurement of the drag. Numerical values of the drag were completely outside of the calibration curve provided by the manufacturer of the balance.

Nevertheless, by examining figures 5 and 6, the agreement is very good especially for the lift curves, even at Re = 42,000. This means that our methodology is correct, as far as we pay attention to the drag measurement. In the near future, the strain gauge for the drag will be re-calibrated for the appropriate range of drag values.

III. LASER DOPPLER VELOCIMETRY RESULTS

The flow field around the airfoil was analyzed by laser Doppler velocimetry (LDV). Although a completely transparent test section has been manufactured at the laboratory, preference was given to the on-axis backscatter set up. The reason for this was its superior easiness regarding the alignment of emitting and of receiving optics as compared with forward scattering. A lower scattering in the backward position of the receiver was not an issue because of the availability of an adequate seeding device.

The two-dimensional Eppler 61 airfoil was tested at different Reynolds numbers keeping the angle of attack equal to zero.

Before the measurements were started, a grid was drawn in order to locate the points at which the measurement would be performed. Grid points were selected as close as possible to the airfoil surface. We were able to approach the airfoil as close as 2 mm. This was done in several longitudinal and transversal planes.

Reliable statistical data associated with acceptable data rates require about 4,000 samples at each mesh point resulting in measurement times between few milliseconds to ten seconds depending on the local particle concentration.

We now calculate the velocities at 2,830 locations and zero angle of attack. Post processing of the data was achieved with Matlab 5.3.

Figure 7 gives a representation of the velocity vectors around the airfoil. This visualization allows seeing whether the flow follows correctly the shape of the airfoil or has a tendency to separate. The size of each vector gives a qualitative information on the velocity magnitude.

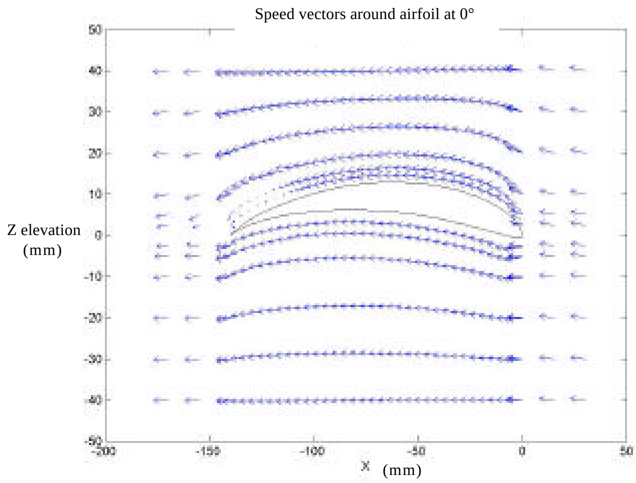

Figure 7 : Vector representation around airfoil at Re 42 000

Such vector plots indicate an important upwash of the streamlines in front of the airfoil leading edge.

Figure 8 gives a quantitative information on the flow field velocity.

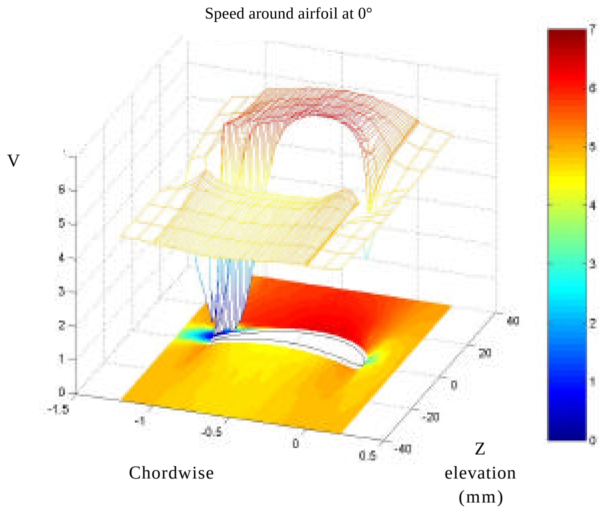

Figure 8 : Speed distribution at Re 46,000

IV. PRESSURE MEASUREMENTS

Another tool to assess the quality of a wing section is to measure the pressure distribution over a range of angles of attack. An instrumented Eppler 61 airfoil is shown on figure 9. On either surface the pressure is measured in 20 stations using a reference transducer and a scanning valve (figure 10). This is a mechanical system which houses a single transducer and sequentially switches up to 48 different incoming pressures to be read by the transducer.

Figure 9 : Profile instrumentation

Caution must be taken for both plugs and leaks. A plug will show as a very slow response to a change in pressure. A leak will show as a change in pressure after a pressure is applied to the model pressure port and held.

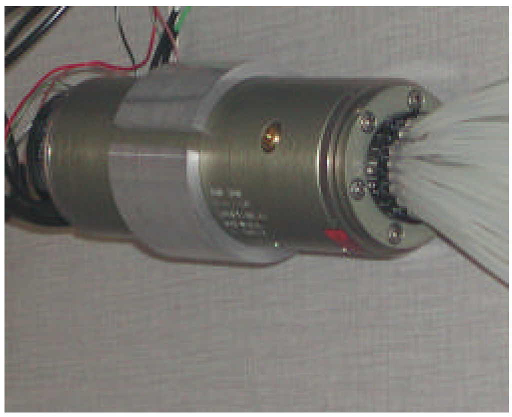

Figure 10: Scanning valve

A typical pressure distribution is shown on figure 11.

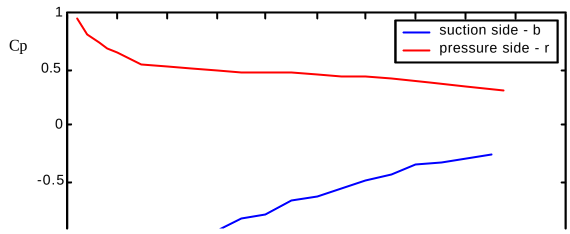

V. CONCEPTUAL DESIGN

A. *From fundamental studies to a micro vehicle…*

Based on the above mentioned experimental tools several profiles have been studied. This permitted to freeze a conceptual design of a MAV (figure 12).

As mentioned in the introduction, a mini/micro aerial vehicle has the only restriction to be easily operated by one individual. We oriented our research towards a bi-plane concept in order to benefit from the vortex induced drag reduction, and obtain an acceptable lift-to-drag ratio. The initial global architecture is presented on figure 12.

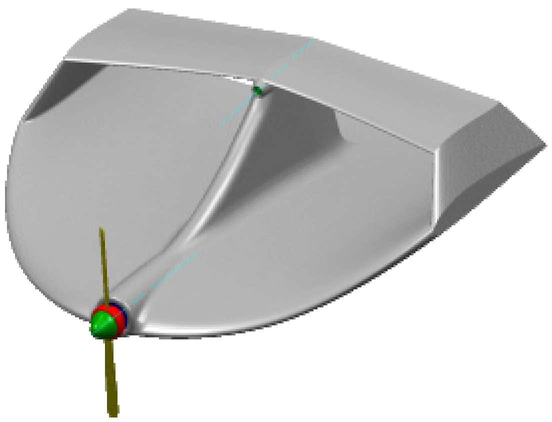

Figure 12: *MIRADOR*, a general design for fixed wings micro aerial vehicle

MIRADOR stands for MicRo Aerial Demonstrator Onera Rma. A very low aspect ratio wing can fly safely at a wide range of angles, and is easier to trim. The range of angles of attack is wider and gusts have less influence. This is the reason why we designed a vehicle with an aspect ratio less than unity.

As visible on figure 12, the shape of the bottom wing is between circular and elliptical. Mathematical analysis and experiments show that the only type of wing that will produce, at all speeds, constant downwash and a load distribution exactly matching the area is one with elliptical planform distribution. The effective angle of attack and the maximum lift coefficient are constant along the entire span.

Another characteristic of this architecture is the progressive dihedral of the bottom wing. Actually, the steeper dihedral of the outer wing panels, acting on a greater moment arm from the centerline of the aircraft, has a powerful stabilizing effect. Moreover, it has been claimed by professor Eppler [4] that the minimum vortex-induced drag for a wing of given span is obtained with dihedral following a circular or elliptical curve, flat at the center and turning gradually more upwards towards the tips.

In order to cover the low Reynolds number range, we decide to use the MH60 airfoil section, considered as a low speed profile.

Arguments in favor of this kind of architecture are:

- compatibility with 150 mm dimensions
- high structural resistance,
- large volume available for equipment layout,
- reduction of the wing tip vortices and therefore of the profile drag
- reduction of the vortex induced drag

We decided to equip the vehicle with off-the-shelf components. These consist of:

- the propulsion system including a propeller, a brushless motor and two electrical batteries
- the vehicle structure made of polyurethane foam and carbon fiber
- a navigation camera, looking in front of the vehicle
- an observation camera (payload) fixed under the vehicle to have the best aerial view possible
- some electronics cards for data link, avionics, payload management
- two servo mechanisms for trim and control

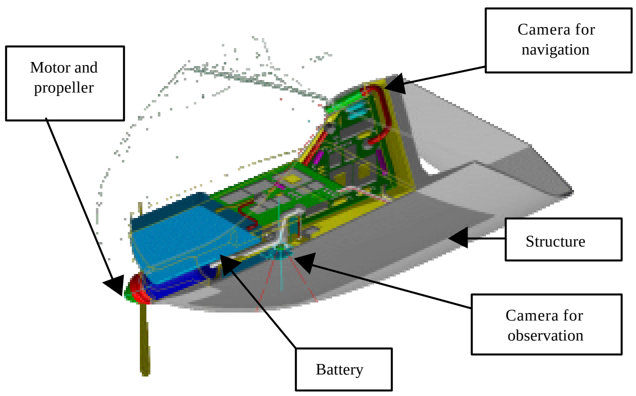

Figure 13: View of internal vehicle organization

The electrical power source is a Lithium Polymer rechargeable battery, produced by ULTRALIFE Inc. This battery is flat, very thin (less than 5 mm) and the shape can be adapted to the design which ensures easy adjustment of the gravity center position.

Such a vehicle would have a global mass of 90 grams, with more than 50 grams occupied by the propulsion system and power supply.

B. Performance analysis

An aerodynamic database has to be built in order to estimate the performance of the aircraft. As numerical data are not yet available due to a lack of correct validated algorithms at low Reynolds numbers and memory capacity, the only way to collect information is by making experiments. An aerodynamic full-scale model (figure 14) is machined by ONERA

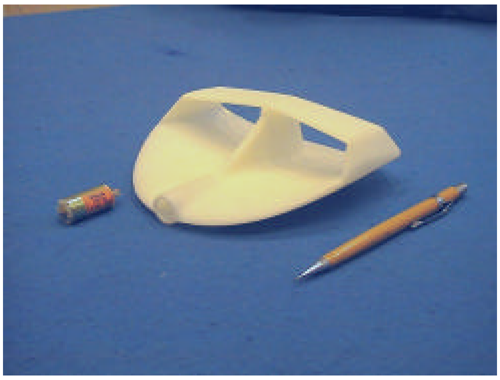

Figure 14: Full-scale model for aerodynamic characterization

An insert is hollowed in order to incorporate the motor and propeller while testing the vehicle in the wind tunnel. A direct thrust-to-drag ratio can be computed, and the interaction between the rotary movement of the propeller and the vehicle can be analyzed.

How supporting the model in the wind tunnel was problematic. There are different ways (figure 15) to do so, but the minimization of the aerodynamic effect should not be overlooked. The first one is a vertical sting, while the other one is parallel to the flow.

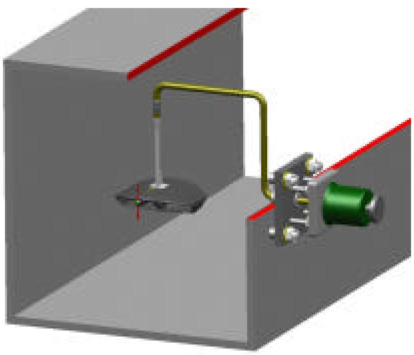

Careful comparison of the drag coefficients for those two configurations (figures 16 & 17) leads to the choice of the vertical support. Actually, the main reason is the reduction of vibration even if the drag coefficient is a little higher.

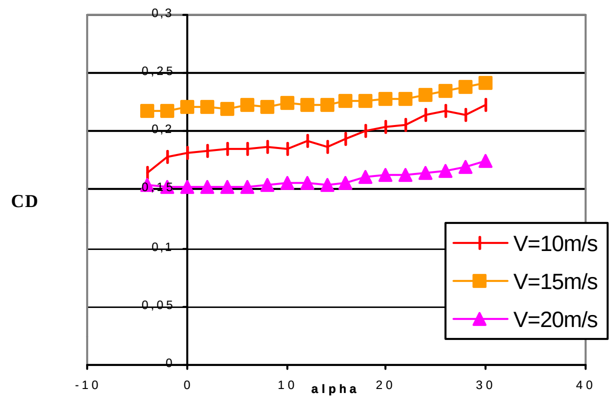

Figure 16: Characterization CD of horizontal sting

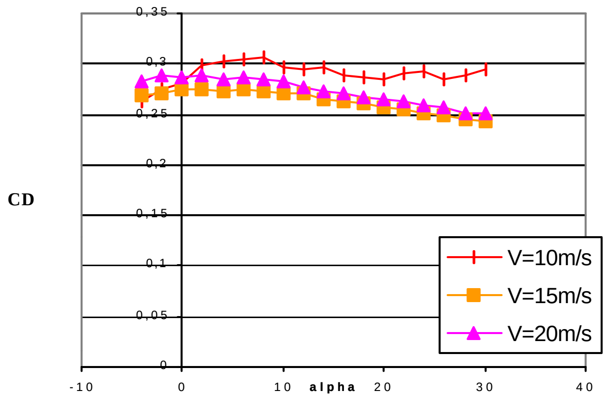

Figure 17: Characterization CD of vertical sting

The support influence being removed, the characteristics of the vehicle itself can now be determined. We obtained a complete aerodynamic database (figures 18 & 19) for the flight domain of interest. Flow speed varied between 5 and 25 m/s while the angle of attack changed from –4° to 30° in order to reach the stall angle.

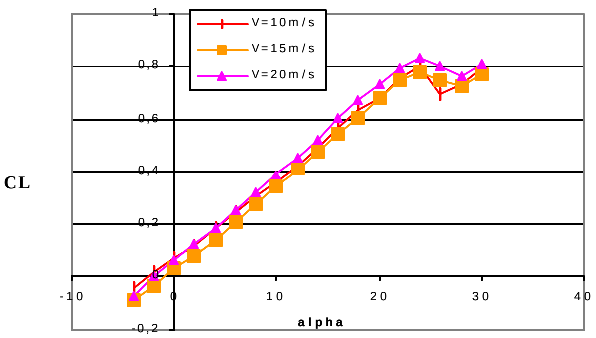

Figure 18: Lift coefficient measurement function of angle of attack

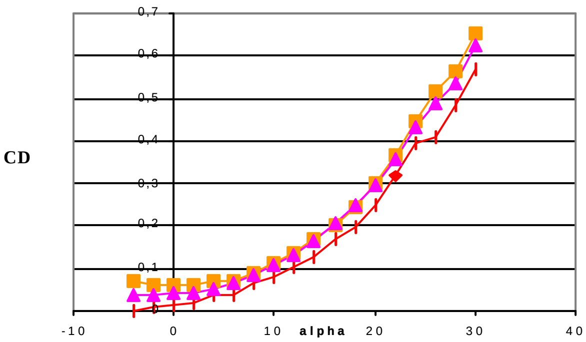

Figure 19: Drag coefficient measurement function of angle of attack

We notice the weak stall slope at an angle of attack of 24 °. This gives a wide range of angles available and is useful in order to avoid loosing total control of the aircraft at the stall angle. The maximum lift coefficient is around 0.8 while the highest drag coefficient is 0.6. The slope of the pitching moment is negative at all speeds while the zero value is not always positive. The vehicle is relatively stable, and specifically designed for some speeds. Lift-to-drag ratio attains a maximum value of 5 at an angle of attack of 8°.

This database is then implemented in a performance code. In a first step, this code was used to design the propulsion system, and especially to optimize battery, electrical motor and propeller. Indeed, energy is a major problem in this micro vehicle if we want to obtain flight endurance greater than a few minutes. To have a good autonomy, we optimized the global propulsion system (battery + motor + propeller) and not only one of these three components (figures 20 & 21).

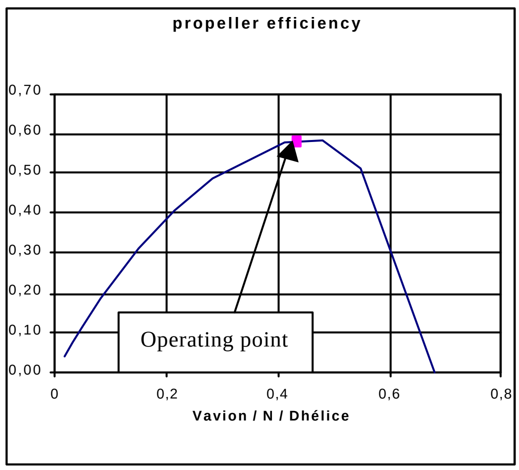

Figure 20: Propeller Efficiency

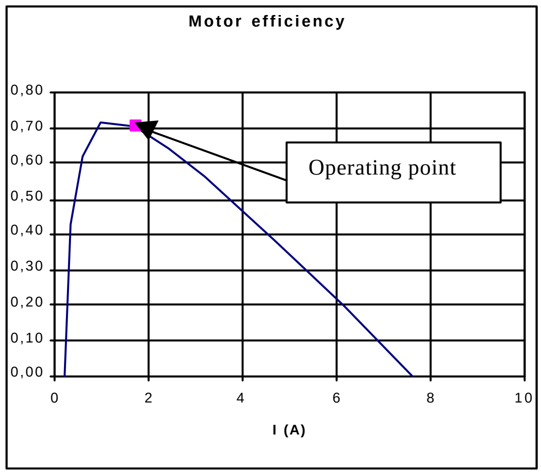

Figure 21: Motor Efficiency

We completed the experimental investigation with the integration of propulsion components in the RMA wind tunnel. In the near future we will complete these results by using optical diagnostic tools such as LDV, PIV and flow visualization techniques (figure 22).

We have also started a numerical simulation approach to complement the experimental work. The first activity is to simulate the bi-plane wings to analyze aerodynamic interaction effects and, eventually, optimize size, stagger, gap ... between the wings.

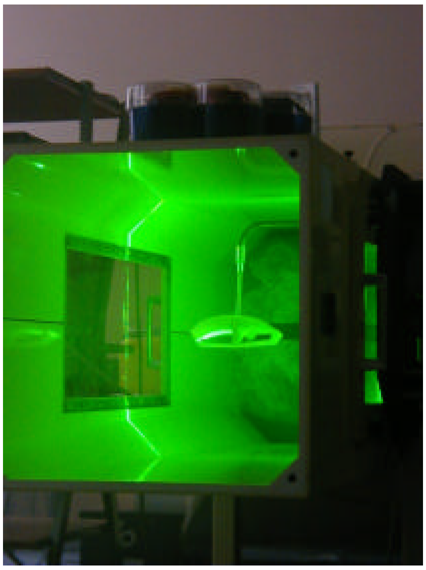

Figure 22: Scale model laser visualization in wind tunnel

C. Flight is reality

To confirm these experimental results, we are aware that we need to execute realistic flights. It's the only way to verify all experimental or theoretical results. In addition, it's a very good objective to stimulate the team working around the project.

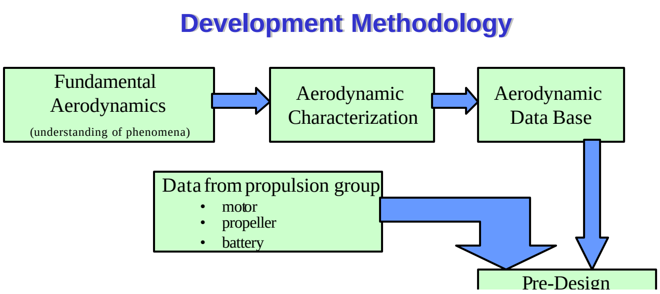

In order to minimize cost, arrive quickly to the flight tests and be able to change something easily during the development phases, we decide to have a non-integrated solution using only "off-the-shelf" components. The same vehicle is also designed at the "5/3"-scale. A standard propulsion system was adapted, based on Lithium polymer rechargeable batteries (but with a standard design) and a brushless motor equipped with propeller. The total mass of that vehicle is around 200 grams with more than 75% for the propulsion system (motor and power source) (figure 24).

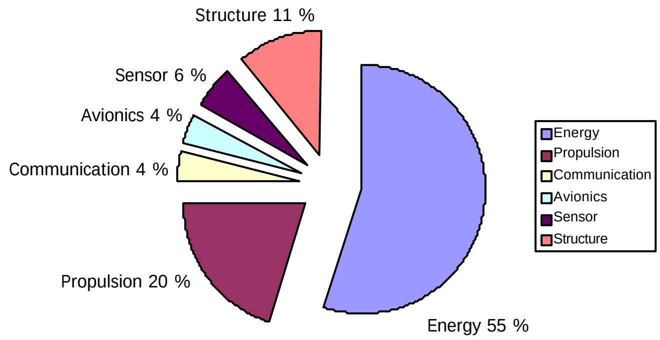

Figure 24: Weight distribution for 250mm scale-model

database, propulsion model,…). In a first step, we will have no payload on board and the first flight will be remotely piloted. Nevertheless, our own experience with this size of vehicles is that they are very difficult to control without stabilization system. That is the reason why we equipped the vehicle with a pitch-roll stabilization system (2 axis –figure 25). The stabilization system has already been successfully tested on other kinds of vehicles. This system is an optical device, it has only day capabilities but is cheap and its sensitivity is easy to adjust.

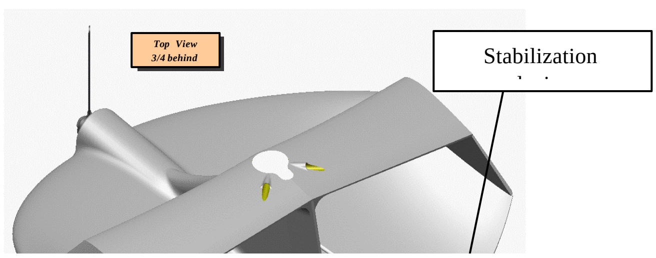

The theoretical performances for this vehicle are more than 30 min at 12 m/s (optimal cruise speed), and we hope to have around 20min for a realistic trajectory. The angle of attack at optimal speed is 8°, broadly under the angle of stall what ensures a safe flight.

VI. CONCLUSION

We can now say we have good knowledge and tools in the different measurement techniques at low Reynolds numbers. The results obtained in our wind tunnel facilities being in good agreement with those performed at University of Notre Dame, we are confident in our technique.

The scientific processes allow to determine what should be the best design without too many trial and error iterations.

The optima for stagger and gap for the bi-plane are still being studied.

Finally, an innovative conceptual design, for good stability and control, low speed flight is born. This vehicle is supposed to take to the air very soon.

REFERENCES

[1] D. Greenblatt and I. J. Wwygnanski – Use of Periodic Excitation to enhance Airfoil Performance at Low Reynolds Number – J. Aircraft vol 38 n°1

[2] T. J. Mueller – Aerodynamic Measurements at Low Reynolds Numbers for Fixed Wing Micro Air Vehicules – RTO EN – 9 september 1999

[3] J. B. Barlow, W. H. Rae Jr A. Pope – Low Speed Wind Tunnel Testing – Wiley Interscience Edition 1999

[4] M. Simons – Model Aircraft Aerodynamics – Fourth Edition